

# Strain gauge measurements of carbon fiber Dee for the CMS Phase-2 Upgrade of the Tracker Forward Pixel Detector

Diyaselis Delgado López  
*University of Puerto Rico, Mayagüez, PR*  
(Cornell University, CMS Collaboration)  
(Dated: August 12, 2019)

The silicon sensors of the TFPX are mounted on a carbon fiber structure called “Dee”, due to its shape; it experiences deflection, upon thermal expansion and contraction of the material, and that deflection is measured by a strain gauge using a Dee prototype upon an applied load. The project entails the selection of a design for a strain gauge experiment to measure deflection and failure in carbon fiber used in the Dee. Based on the acquired data, a material profile for carbon fiber is used as a guideline for the Dee’s construction and modeling as part of the Phase-2 Upgrade of the Forward Pixel Detector from the CMS Experiment.

**Keywords:** Strain Gauges | Carbon Fiber | TFPX | CMS | Mechanical Stress | Cantilever Beam Bending Test | Thermal Stress | Thermal Shock

## CONTENTS

I. Introduction	42	ratio is the ratio of transverse contraction strain to longitudinal extension strain in the direction of a stretching force [1]. These properties will help determine the strain, the amount of deformation of a body due to an applied force, of each of our testing samples. As a control sample, the strain properties of Aluminium 3003 were considered for the part. Aluminium 3003 is a popular alloy of aluminum-manganese; it’s used as a reference material since its properties are already well known and established, so it would help calibrating the strain gauges for this experiment. Aluminum 3003 has a Youngs modulus of 70-80 GPa and a Poissons ratio of 0.33 [1]. The project focuses on testing the strain properties of a carbon-carbon composite, the leading material for the construction of the Dee’s of the CMS Tracker Forward Pixel Detector. Carbon fiber is a unique material due to its intricate layers and direction of carbon fiber tubes upon construction, which makes the effect of stress and strain on carbon fiber materials change with the direction which it is applied. The carbon fibers themselves are much more brittle than metal, but the matrix of the carbon fibers allows for one individual carbon fiber to fail without the failure of the entire piece due to surrounding fibers compensating for the failure. Carbon foam is then glued and cured as an intermediary layer of the carbon fiber Dee, which changes the Poisson ratio of the total material, but in fact resulting in a more sturdy composition overall.
II. Design of Carbon Fiber Strain Test: Mechanical Stress	44	
III. Strain Gauge Selection	45	
IV. Implementing Cantilever Beam Bending Test	46	
A. Strain Gauge Application	47	
B. Experimental Testing	48	
V. Design of Carbon Fiber Strain test: Thermal stress	49	
A. Thermal Shock Testing	50	
VI. Results	51	
A. Half Wheatstone Bridge Configuration	52	
B. Full Wheatstone Bridge Configuration	53	
C. Thermal Expansion	54	
VII. Conclusions	55	
VIII. Recommendations	56	
References	57	
IX. Appendix A: Strain Gauge Installation	58	
X. Appendix B: Thermal Expansion Results	59	
	60	
	61	
	62	
	63	
	64	
	65	
	66	
	67	
	68	
	69	
	70	
	71	
	72	
	73	
	74	
	75	
	76	
	77	
	78	
	79	
	80	
	81	
	82	
	83	
	84	
	85	
	86	
	87	
	88	
	89	
	90	
	91	
	92	
	93	
	94	
	95	
	96	
	97	
	98	
	99	
	100	

## I. INTRODUCTION

During the testing of the materials, some of the properties of interest are the Young’s modulus and the Poisson’s ratio. Young’s modulus refers to the numerical value of the elastic property of a material, which represents the ability to deform the material. The Poisson’s

While there are several methods of measuring strain, the most common is with a strain gauge, a tool whose electrical resistance varies in proportion to the amount of strain in the device [2]. The Wheatstone bridge, illustrated in Figure 1, is the most used circuit to measure strain of an applied strain gauge, as the circuit can be employed to easily calculate an unknown strain by mea-

79 suring the voltage difference between two ends of a simple  
80 bridge. The change in voltage is then related to a change  
81 in area of the gauge by a gauge factor defined by the  
82 manufacturer of the strain gauge.

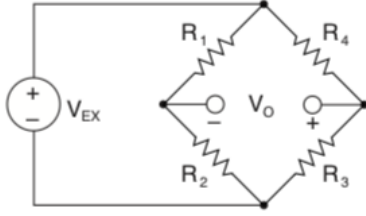


FIG. 1. **Wheatstone bridge circuit.** The Wheatstone bridge schematic has four elements arranged in a diamond pattern, with an excitation voltage from a power source, while the output reading is usually, taken across the midpoint [3].

83 When testing our materials, there are two types of  
84 measurements, axial strain and bending strain in Figure 2,  
85 that could be taken. Axial strain is caused when a  
86 material is pulled along an axis parallel to the material,  
87 which stresses both sides of the material equally. Bending  
88 strain is caused when strain is applied to an axis perpendicular  
89 to the material, therefore causing one of the faces  
90 of the material to undergo compression and the other,  
91 expansion.

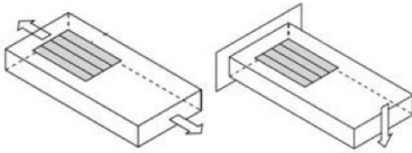


FIG. 2. **Types of Strain.** Axial strain measures how a material stretches or pulls apart. Bending strain measures a stretch on one side and a contraction on the other side [2].

92 A proposition for testing the strain of the carbon fiber  
93 is the Cantilever beam bending test, as shown in Figure 3.  
94 It involves a simple mechanical experiment that is able to  
95 show the basic material properties of the sample material.  
96 A load is placed at the end of the beam, creating a bend  
97 in the material that is then measured by the change of  
98 resistance in the attached strain gauges. By using both a  
99 half and full Wheatstone bridge configurations of strain  
100 gauges on the cantilever beam, both the Young's modulus  
101 and Poisson's ratio of the material can be found.

102 The equation for strain ( $\epsilon$ ) in the cantilever beam test  
103 depends on the configuration of strain gauges being used.  
104 A fundamental component in this calculation is the voltage  
105 ratio  $V_r$ , which is dependent of the output voltage  
106 taken across the circuit. This can be computed as so:

$$V_r = \frac{V_O \text{ (strained)} - V_O \text{ (unstrained)}}{V_{EX}}$$

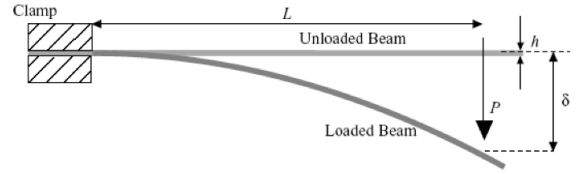


FIG. 3. **Cantilever beam bending test**

107 where  $V_O$  (strained) is the measured signal voltage  
108 when strained, and  $V_O$  (unstrained) is the initial, un-  
109 strained output voltage.  $V_{EX}$  is the excitation voltage  
110 applied by the power source. For each of the configura-  
111 tions used, half and full Wheatstone bridge, the strain  
112 gauge equations differ.

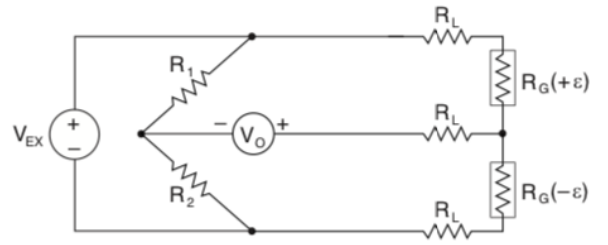


FIG. 4. **Half Wheatstone Bridge.** In this case, the Half Bridge consists of two individual resistors,  $R_1$  and  $R_2$ , and two gauges that would take the place of  $R_3$  and  $R_4$  on the circuit.

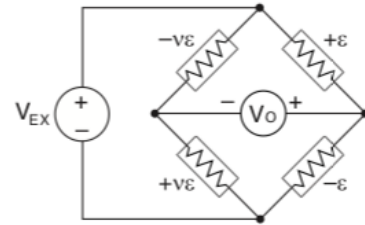


FIG. 5. **Full Wheatstone Bridge.** The Full Bridge consists of two gauges representing  $R_3$  and  $R_4$ , and two gauges that are aligned perpendicular to the main axis as  $R_1$  and  $R_2$  on the circuit.

For the Half Wheatstone bridge, shown in Figure 4, the circuit is completed with external resistances and for this specific design and positioning of the strain gauges, the strain equation becomes:

$$\epsilon = \frac{-2V_r}{GF} \cdot \left(1 + \frac{R_L}{R_G}\right)$$

and for the Full Wheatstone Bridge of Figure 5,

$$\epsilon = \frac{-2V_r}{GF(\nu + 1)}.$$

In this context,  $R_G$  is the nominal resistance value of the strain gauge, GF is the gauge factor of strain gauge, and  $R_L$  is the lead resistance throughout the wires. Also, the designation  $(+\epsilon)$  and  $(-\epsilon)$  indicates active strain gauges mounted in tension and compression (i.e. top and bottom of beam), respectively. The designation  $(-\nu\epsilon)$  indicates that the strain gauge is mounted in the transversal direction, so that its resistance change is primarily due to the Poisson's strain, whose magnitude is given as  $-\nu\epsilon$  [3].

The stress of the beam is given by the following equation:

$$\sigma = \frac{M_x y}{I_x}$$

where  $\sigma$  is the stress,  $I_x$  is the moment of inertia along a neutral axis,  $y$  is the perpendicular distance, and  $M_x$  is the second moment of area along  $x$ . In practice, the stress equation can be modified in terms of the force applied and the dimensions of the test samples,

$$\sigma = \frac{6Wx}{bt^2},$$

where  $W$  is the weight or force,  $x$  is the distance between the clamp and the point of the applied force,  $b$  is the width of the beam's base, and  $t$  is the thickness [4]. The values of found stress and strain are then compared in a ratio known as Young's Modulus ( $\Upsilon$  or  $E$ ),

$$E = \frac{\sigma}{\epsilon}.$$

Furthermore, calculations of the Poisson's ratio can be acquired after tests with the Half Bridge gauge circuit. This configuration allows to compute the Young's modulus, a constant that can be implemented in the strain equation for Full Bridge circuits. After solving for the unknown variables in the strain equation, the Poisson's ratio is obtained by the following:

$$\nu = \frac{-2EV_r}{GF(\sigma)} - 1.$$

### III. STRAIN GAUGE SELECTION

The selection of the strain gauge befalls after the consideration of the following factors: compensation, sensitivity, covering agent constraints, carrier material, gauge length, and cyclic endurance. Strain gauges are extremely sensitive to changes in temperature as they respond to a change in resistance in the gauge. Provided on typical strain gauge documentation are compensation functions to adjust the measured strain to its actual value. Different strain gauges are more or less sensitive to strain due to the materials used in their own construction. Strain gauges are made with thin parallel wires, and their measurements depend on the resistance change due to the elongation or shortening of the wire due to strain.

Moreover, the correct covering agent must be chosen for the specific project using the strain gauge, in this case, it has been chosen Kapton tape. If an incorrect covering agent is used, the wires used to measure the strain on the gauge can be damaged, causing the measurement to be incorrect. Also, the covering agent can affect how far the gauge is allowed to bend which changes the resistance measurement on the gauge. The carrier material of the gauge provides a good electrical insulation between the wires of the strain gauge and the sample, it allows for a base Poisson ratio on which to place the measuring wires. Selecting the correct Poisson ratio of the carrying strip of material ensures that the carrier of the gauge does not influence the measurement of resistance of the gauge and allows the information from the gauge to be as noiseless as possible. Additionally, gauge length must be selected as to ensure the measurement is both not averaged over too large of the area of the test material and not a measurement of only one part of the test piece. Depending on how many tests are occurring with the same gauge, cyclic endurance of the gauge must be accounted for to ensure the measurement remains accurate over time. Finally, the geometry of the inner wires of the gauges would determine the most appropriate tool to use. Linear strain gauges are excellent for finding the strain on a rectangular piece with known stress strain principle axes, but on pieces that are not regular, they can be hard to get correct measurements with. After deliberation, the rectangular rosette was used to find the principal strains and their orientation. The gauges selected show a combination of displaced grids by  $45^\circ$ , in which can detect deflection within its  $0^\circ$ ,  $45^\circ$ , and  $90^\circ$  directions, as depicted in Figure 6a. This trait is helpful when dealing with the carbon fiber as they're configured with different displaced layers.

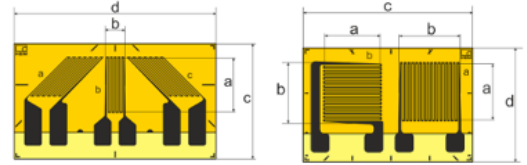


FIG. 6. **Strain Gauges.** (a) A 3-grid gauge of  $45^\circ$  separation with a resistance of  $120 \Omega$ . (b) A 2-grid gauge of  $90^\circ$  separation with a resistance of  $350 \Omega$ .

Apart from the gauges themselves, the data acquisition (DAQ) system will be used to interpret voltage difference between each arm of Wheatstone Bridge. The system needs proper instructions for wiring and configuring the DAQ device for strain gauge measurements. A LabVIEW program has been made programs for several strain gauge configurations based on their setup; it can then be modified for this project easily. Using the program, the data logger can measure DC voltage across the Hi and Lo connections of one channel in the module.

## IV. IMPLEMENTING CANTILEVER BEAM BENDING TEST

### A. Strain Gauge Application

The conditions for the installation of the strain gauges begins with cleaning the work space and all components being used with acetone. When preparing the sample materials, sanding the surface lightly proved to help create a slight texture for the epoxy to hold the gauge in place. Before mixing the glue, the samples were marked to make sure the alignment matches with the axis of the gauges. Then, handling with great care, the strain gauges were removed from the packaging and placed on a clear film with cellophane tape on top to create a handle for better grasp of the gauges (see Appendix A for reference pictures of the installation). Following the directions of the epoxy's manufacturer, a mixture of one part dry with 5-6 drops of liquid, the X60 adhesive was applied to the bottom of exposed gauge, where it would meet the surface of the material. To ensure the gauge would hold, it was pressed down with the thumb for a recurrent time of 5 minutes as the epoxy hardens. Before soldering to the solder pads, again scratching lightly the surface of the pads will make the soldering stick better. Using lead wires, each of the six connections were soldered and tested by measuring their proper resistance. The resistance of the gauges is a set value from the manufacturer, and so, to measure said resistance the gauges behave as a resistor as the first three wires are connected together against the last three. With a multimeter the ground connection is attached to one end and the active connection is hooked to the other end of the gauge wires. Finally, after wires are attached, the top of the gauges was taped with cellophane tape (i.e. Kapton tape) to provide some strain relief.

### B. Experimental Testing

To begin the test runs, after applying the strain gauges, both half and full Wheatstone bridge circuits were used to measure the properties of both the aluminum 3003 and carbon fiber-foam. The carbon fiber-foam was tested with weights of less mass due to its lower failure point. Furthermore, fiber failure, caused by individual carbon fibers breaking, lower the possible load of the whole material piece since each fiber broken must be compensated by another. Also, failure in the epoxy, used to glue the individual sheets of carbon fiber together, results in the failure of the overall sheet as well. Following said failure, delamination occurs, which is the process by which the sheets peel apart from failure of the glue holding them together, leaving the material inoperative. The test involved clamping the material by one end, experimentally the sample was held by a wooden plate on top of it, tightly secured by to clamps, illustrated in Figure 7.

As depicted on the previous figure, after the beam's

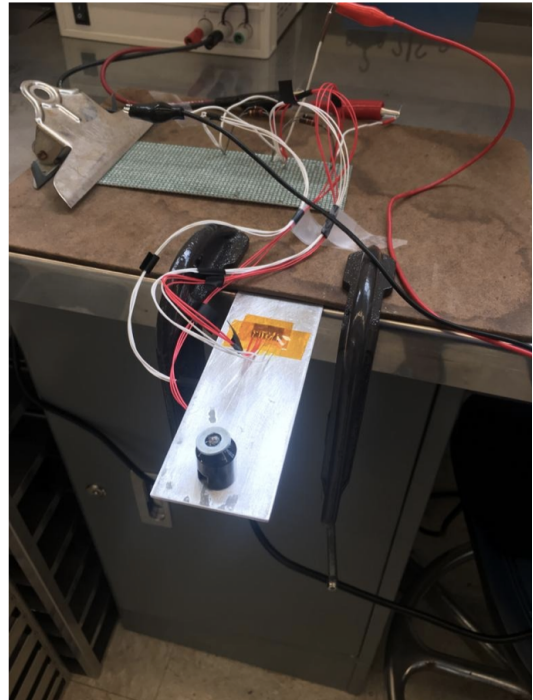


FIG. 7. Cantilever Beam Bending Test Setup

setup was achieved, the experiment was ready for testing. Consequently, masses, in gradual increments of 10 grams, were placed to the opposite end of the beam and data was collected from a voltmeter. With the obtained output voltage, further steps involved calculating the voltage ratio and so, the strain implemented.

## V. DESIGN OF CARBON FIBER STRAIN TEST: THERMAL STRESS

The thermal expansion coefficient is another physical property considerably important in mechanical and structural design applications of a material, in this case, the carbon fiber as a main structure of the TFPX detector. When a strain gauge is installed on a stress-free sample and the temperature of the material is changed, the output voltage from the gauge changes as well, hinting that the material is being strained. This effect is referred to as temperature-induced apparent strain [5]; it is caused by a combination of two factors: the resistivity of the gauge changes with temperature and also an additional resistance change occurs due to the different thermal expansion coefficients of the gauge and the test material to which it is bonded [6]. Within the documentation provided from the the gauges selected, there's a strain compensation equation for each specific gauge. For the 3-grid gauge, mainly used in the experiment, said equation is:

$$\epsilon_s(T) = -21.0 + 2.48 \cdot T - 8.14 \cdot 10^{-2} \cdot T^2 + 3.13 \cdot 10^{-4} \cdot T^3$$



Said equation will be added to the temperature-induced apparent strain formula, as shown below, to examine the real strain in the test sample.

$$\epsilon = \frac{\alpha}{GF} + (\beta_s + \beta_g)$$

### A. Thermal Shock Testing

For these series of test runs, after applying the strain gauges, both half and full Wheatstone bridge circuits were used to measure the thermal properties of both the aluminum alloy and carbon-carbon composites. Among certain expected behaviors is failure of the epoxy, as it would help understand the delamination observed in other circumstances. Under higher temperatures, the thermal stress of the material leaves significant damage in the result carbon fiber-foam composition. The thermal shock test involved placing the material in an oven and heating it up. As the material's temperature rises, changes in the output voltage of the gauges is documented. The experimental setup is composed of the oven, thermocouple, long wires, and a circuit board connected to the DAQ system, as illustrated in Figure 8.

The temperature changes would range between 30 °C and 110 °C. Consequently, the temperature will gradually increase by 10 °C, as permitted by the oven in use, and stay within a constant temperature over 3-5 minutes. Data was collected from the data logger and with the obtained output voltages the voltage ratio and the apparent strain were calculated.

## VI. RESULTS

Results of the Cantilever experiment were initially collected from the DAQ system stationed at the CMS Lab. The data logger was programmed to process the input voltage from the power supply and the output voltage across the circuit. From these measurements, calculations for the voltage ratio, strain, stress, and finally, Young's modulus.

### A. Half Wheatstone Bridge Configuration

To start with the tests, the first sample was an aluminum beam with the following dimensions:

TABLE I. Dimensions for the Aluminum 3000 beam.

Length [mm]	Width [mm]	Thickness [mm]
154.5	44.8	1.4

Another important proportion is the distance between the clamp to the point where the force is applied, in this case, where the mass is placed. For the aluminum, said distance was measured to be 122.2 mm. Using the 3-grid



FIG. 8. **Thermal Shock Test Setup.** (a) Material samples and thermocouple place inside the oven. (b) Electrical connections of the circuit and DAQ system.

gauges of 120  $\Omega$  resistance in a half Wheatstone bridge configuration, wires with lead resistance of 12  $\Omega$ , and an initial source voltage of 0.5 V, approximately, test results are portrayed below.

TABLE II. Strain-Stress Test Results for Aluminum 3000.

Mass [g]	Strain	Stress [MPa]	Young's Modulus [GPa]
10	1.02e-05	0.82	85.02
20	1.90e-05	1.65	84.99
30	2.52e-05	2.47	99.51
40	3.43e-05	3.29	96.90
50	4.23e-05	4.11	97.15
60	5.23e-05	4.94	95.15
70	6.11e-05	5.76	94.86
80	6.94e-05	6.58	95.48
90	7.52e-05	7.40	99.16
100	8.78e-05	8.23	93.98
110	9.65e-05	9.05	93.57
120	1.06e-04	9.87	93.12

Additionally, to help visualize and understand these calculations, the following graphs plot the data as functions of the inputs. Figures 9, 10 and 11 show the different properties of the Aluminum 3003 tested.

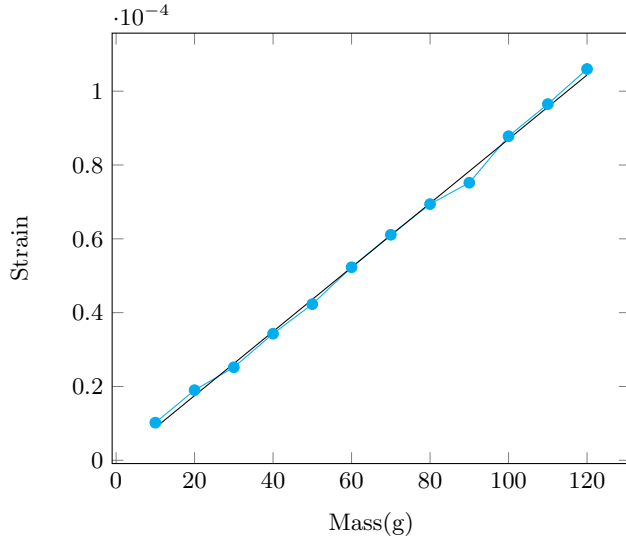


FIG. 9. **Strain vs. Mass.** A linear behavior is observed as the strain is proportional to the mass, indirectly through the stress.

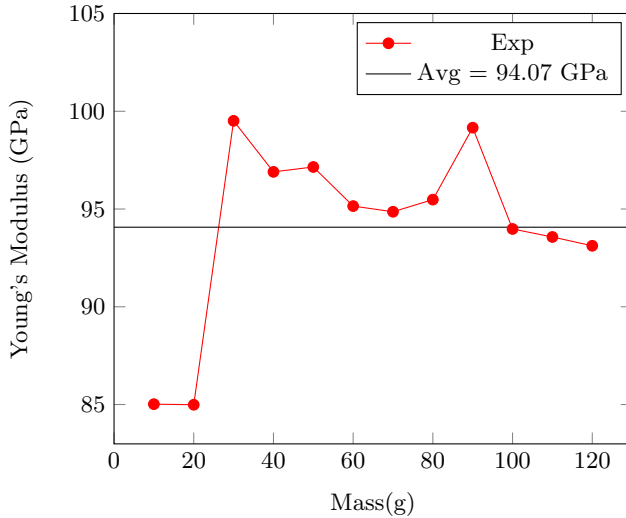


FIG. 10. **Young's Modulus vs. Mass.** A constant behavior should be observed as the Young's Modulus stands for the elasticity modulus, a constant property of materials.

The following sample was a piece of carbon fiber attached to carbon foam only with dimensions of:

TABLE III. Dimensions for the Carbon Fiber-Foam beam.

Length [mm]	Width [mm]	Thickness [mm]
78.2	36.0	2.2

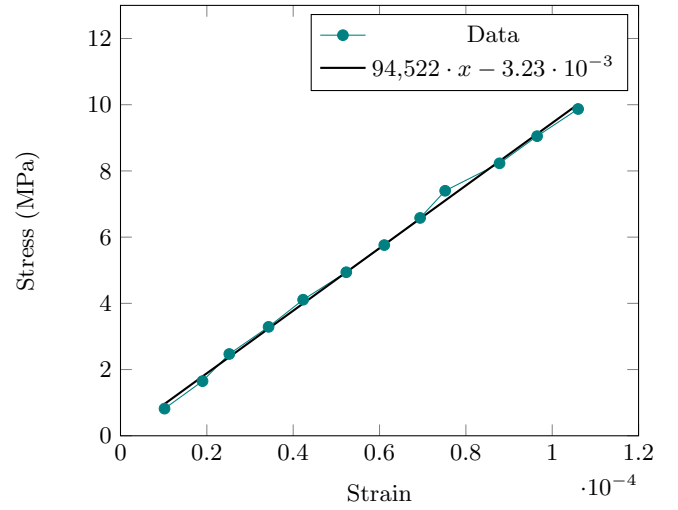


FIG. 11. **Stress vs. Strain.** A linear behavior is observed as the stress is proportional to the strain, as defined by the Young's modulus.

Next, the distance between the clamp to the point where the force is applied, in this case, where the mass is placed. For the carbon fiber-foam beam, said distance was measured to be 65.9 mm. Using the 3-grid gauges of 120  $\Omega$  resistance in a half Wheatstone bridge configuration, wires with lead resistance of 12  $\Omega$ , and an initial source voltage of 0.5 V, approximately, test results for this sample are shown below.

TABLE IV. Strain-Stress Test Results for Carbon Fiber-Foam.

Mass [g]	Strain	Stress [MPa]	Young's Modulus [GPa]
10	2.94e-05	0.22	7.47
20	5.88e-05	0.45	7.58
30	8.66e-05	0.67	7.75
40	1.18e-04	0.89	7.56
50	1.43e-04	1.11	7.79
60	1.73e-04	1.34	7.74
70	2.10e-04	1.56	7.40
80	2.41e-04	1.78	7.39
90	2.73e-04	2.00	7.34
100	2.96e-04	2.23	7.52
110	3.27e-04	2.45	7.51
120	3.67e-04	2.67	7.27

To help visualize and understand these calculations, the following graphs plot the data as functions of the inputs. Figures 12, 13 and 14 show the different properties of the carbon fiber-foam sample tested. Although the Dee for the detector will not have the layer of exposed carbon foam it is a good test to see how the material reacts under mechanical stress.

The final sample was a piece of carbon fiber attached to carbon foam and another layer of carbon fiber with dimensions shown at the Table V.

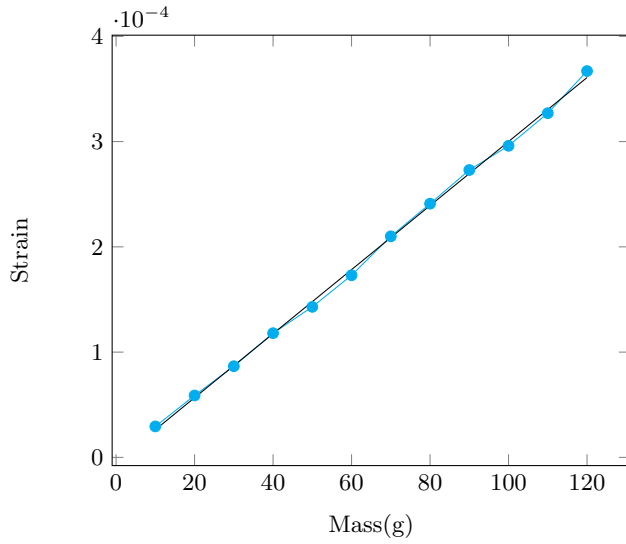


FIG. 12. **Strain vs. Mass.** A linear behavior is observed as the strain is proportional to the mass, indirectly through the stress.

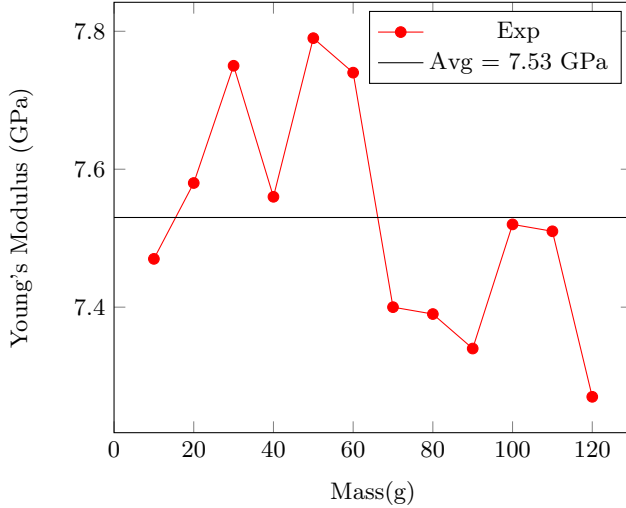


FIG. 13. **Young's Modulus vs. Mass.** A constant behavior should be observed as the Young's Modulus stands for the elasticity modulus, a constant property of materials.

TABLE V. Dimensions for the Carbon Fiber-Foam-Fiber beam.

Length [mm]	Width [mm]	Thickness [mm]
85.8	26.0	2.5

Next, for the carbon fiber-foam beam, the distance between the clamp to the point where the force is applied, in this case, where the mass is placed, is 72.1 mm. Using the 3-grid gauges of 120  $\Omega$  resistance in a half Wheatstone bridge configuration, wires with lead resistance of 12  $\Omega$ , and an initial source voltage of 0.5 V, approximately, test results for this sample are shown below.

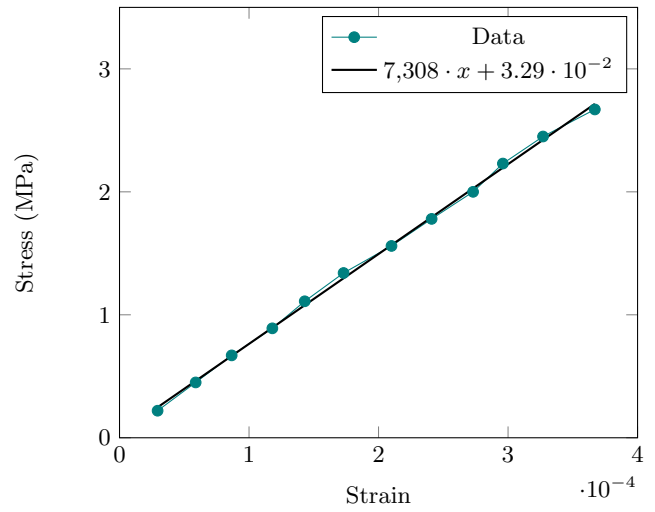


FIG. 14. **Stress vs. Strain.** A linear behavior is observed as the stress is proportional to the strain, as defined by the Young's modulus.

TABLE VI. Strain-Stress Test Results for Carbon Fiber-Foam-Fiber.

Mass [g]	Strain	Stress [MPa]	Young's Modulus [GPa]
10	3.34e-06	0.26	83.18
20	6.59e-06	0.52	79.62
30	8.41e-06	0.78	94.94
40	9.69e-06	1.04	108.46
50	1.23e-05	1.31	106.42
60	1.62e-05	1.57	97.70
70	1.97e-05	1.83	93.06
80	2.12e-05	2.09	98.54
90	2.35e-05	2.35	100.02
100	2.74e-05	2.61	95.46
110	2.90e-05	2.87	99.23
120	3.10e-05	3.13	101.14

Again, to help visualize and understand these calculations, the following graphs plot the data as functions of the inputs. Figures 15, 16 and 17 show the different properties of the carbon fiber-foam-fiber tested.

Depicted on Figures 11, 14 and 17, the stress-strain plots give important information regarding the mechanical properties of the materials. Under the tensile test, the slope turns out to be the Young's modulus of elasticity, this value can then be compared to all the previous results. Every sample had their own characteristic stress-strain graphs, but is possible to organize materials with similar properties, depending on their stiffness, composition, etc. Moreover, after numerous tests, some vital observations arose regarding the residual strain displayed by the carbon fiber-foam sample. Residual stresses are generally present in all of the components, up to some degree. And so, particular tests were set in place to compute the behavior of the gauges concerning the stability and recovery of them as put under stress.

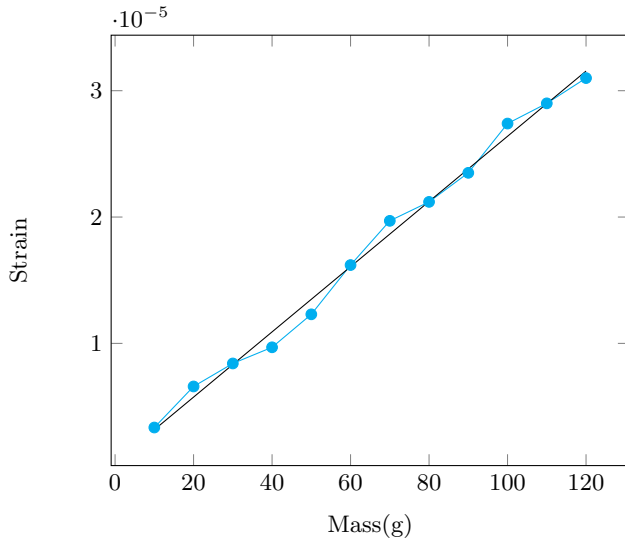


FIG. 15. **Strain vs. Mass.** A linear behavior is observed as the strain is proportional to the mass, indirectly through the stress.

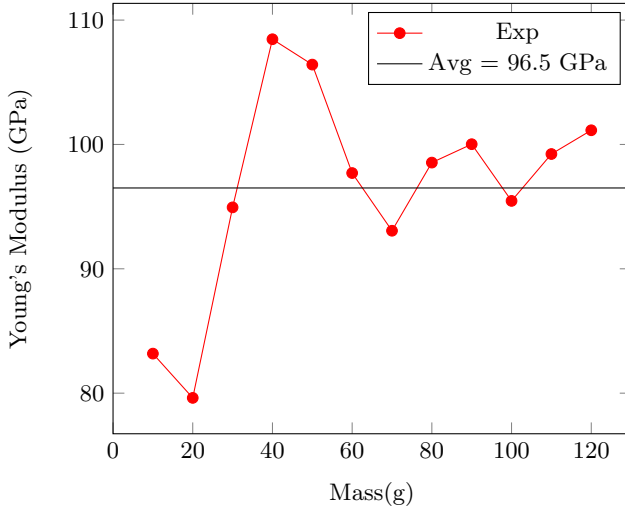


FIG. 16. **Young's Modulus vs. Mass.** A constant behavior should be observed as the Young's Modulus stands for the elasticity modulus, a constant property of materials.

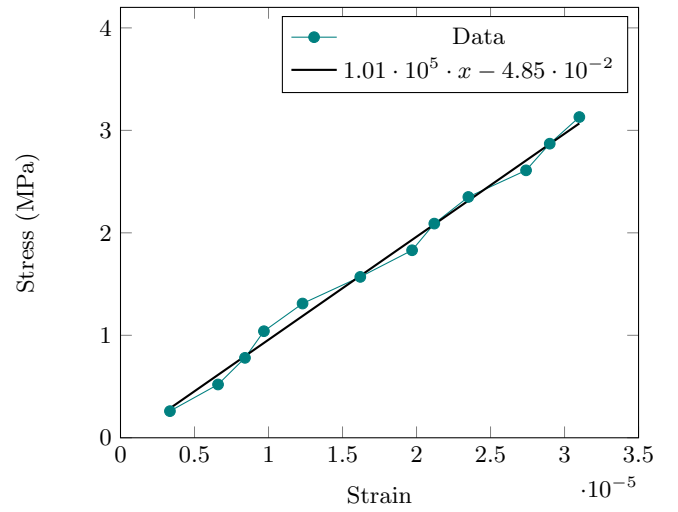


FIG. 17. **Stress vs. Strain.** A linear behavior is observed as the stress is proportional to the strain, as defined by the Young's modulus.

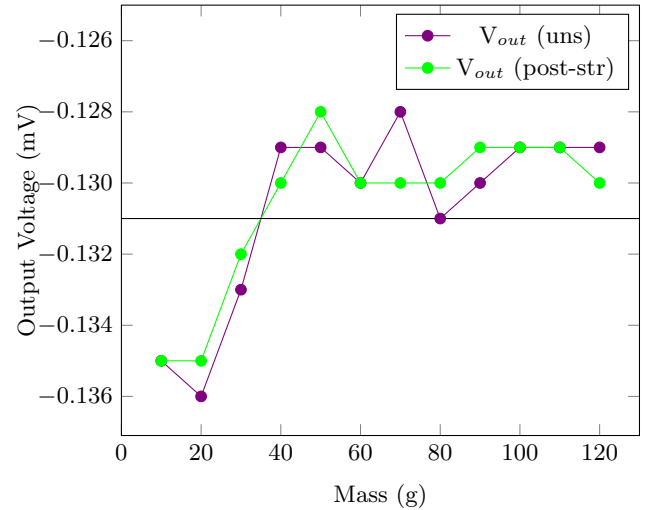


FIG. 18. **Output Voltage vs. Mass.** For the carbon fiber-foam sample, ideally the output voltage across the circuit should remain constant. Recurring average output voltage is -0.131 mV.

Although these results do not show an unchanging output voltage, they were as far best obtained. Another factor to consider is the time period it took for these measurements to stabilize, as shown in Figure 20. Also once strained and relieved, the time period of recovery of the material (i.e. to obtain a similar to the unstrained case.) was measured, as in Figure 21.

Even though the carbon fiber-foam-fiber sandwich did not show any major signs of bending it needed an enormous amount of time to reach stability, compared to the aluminum, for which results were not documented, that quickly settled after visible bents, and yet both are very stiff. This leads to believe that the layer of foam does

carry out the strain for a longer time and it adapts to compensate for that induced stress.

## B. Full Wheatstone Bridge Configuration

The succeeding tests are only feasible after doing the Half Bridge configurations, as previously mentioned. To calculate the strain under this condition the crucial unknown variables are the strain itself and the Poisson's ratio. The sample used for the Full Wheatstone Bridge circuit involves the four 3-grid gauges, two of them glued parallel to the longitudinal main axis and the other two



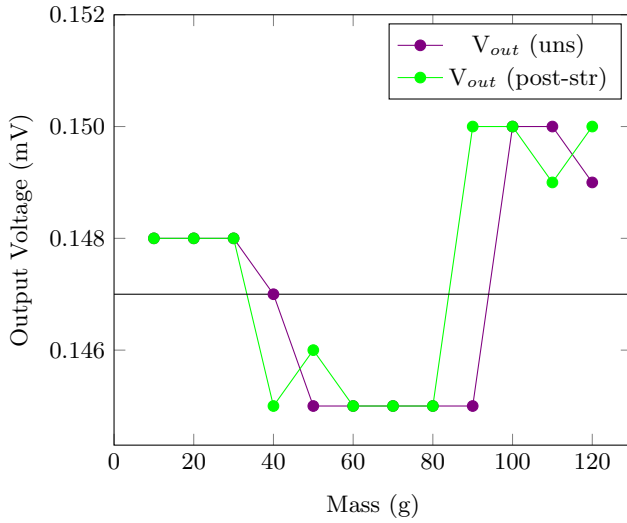


FIG. 19. **Output Voltage vs. Mass.** For the carbon fiber-foam-fiber sample, ideally the output voltage across the circuit should remain constant. Recurring average output voltage is 0.147 mV.

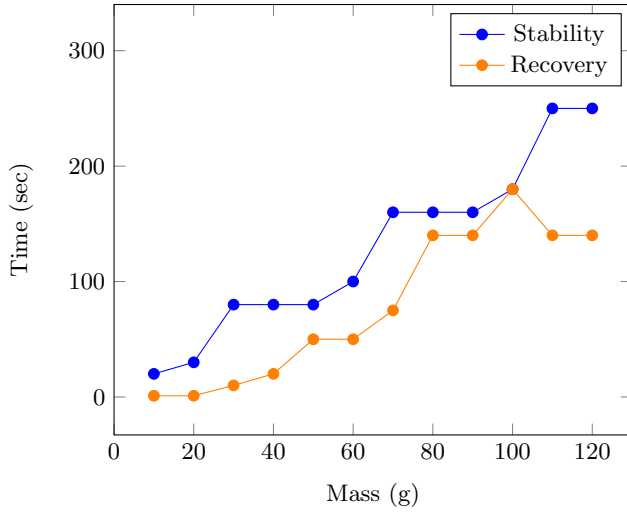


FIG. 20. **Stability-Recovery Time Period.** For the carbon fiber-foam sample, it was expected to show a proportional relation between time and weight, and therefore strain.

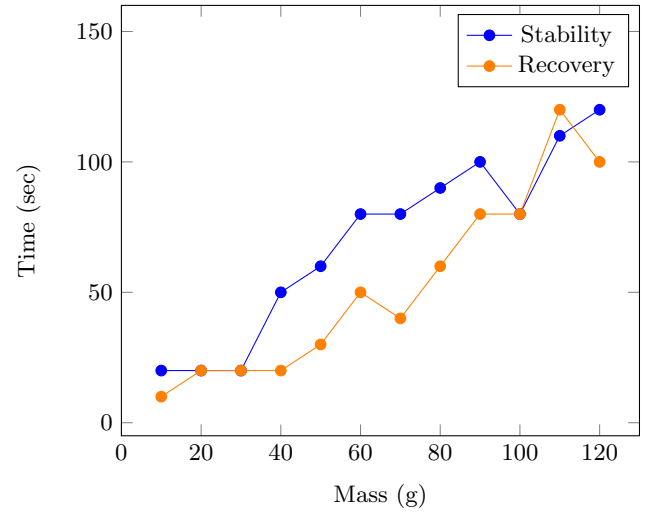


FIG. 21. **Stability-Recovery Time Period.** For the carbon fiber-foam-fiber sample, it was expected to show a proportional relation between time and weight, and therefore strain.



FIG. 22. **Strain Gauges in Full Bridge Formation.** The placement depiction of the gauges as expected for the active/passive gauges in a Full Wheatstone Bridge circuit.

perpendicular to said axis of a carbon fiber-foam piece, as shown in Figure 22. The samples used for Full Wheatstone Bridge involve the two types of gauges described above: an aluminum beam with the 2-grid gauges, a carbon fiber-foam with the 2-grid gauges, and an additional carbon fiber-foam with 3-grid gauges.

The dimensions of the carbon fiber-foam sample are:

TABLE VII. Dimensions for the Carbon Fiber-Foam.

Length [mm]	Width [mm]	Thickness [mm]
150.7	25.6	2.3

Consequently, for the carbon fiber-foam beam, the distance between the clamp and the mass was measured to be 124.8 mm. Using the 3-grid gauges of 120  $\Omega$  resistance in a full Wheatstone bridge configuration, wires with lead resistance of 12  $\Omega$ , and an initial source voltage of 0.5 V, approximately, test results for this sample are shown below.

TABLE VIII. Strain-Stress Test Results for Carbon Fiber-Foam in Full Bridge circuit.

Mass [g]	Voltage Ratio	Poisson's Ratio
10	-8.85e-05	0.27
20	-1.82e-04	0.31
30	-2.75e-04	0.31
40	-3.67e-04	0.31
50	-4.78e-04	0.37
60	-5.79e-04	0.38
70	-6.45e-04	0.32
80	-7.52e-04	0.35
90	-7.76e-04	0.23
100	-9.61e-04	0.38
110	-9.77e-04	0.27

Mass [g]	Strain	Stress [MPa]	Young's Modulus [GPa]
10	6.72e-05	0.54	8.07
20	1.38e-04	1.08	7.84
30	2.09e-04	1.63	7.80
40	2.78e-04	2.17	7.80
50	3.63e-04	2.71	7.48
60	4.39e-04	3.25	7.41
70	4.90e-04	3.80	7.75
80	5.71e-04	4.34	7.60
90	5.89e-04	4.88	8.29
100	7.29e-04	5.42	7.44
110	7.41e-04	5.97	8.05

From these results, the average Poisson's ratio calculated was 0.32. This value was then implemented to the strain equation for computing once again the Young's modulus, resulting in an average modulus of 7.78. Moreover, to help visualize and understand these calculations, the following graphs plot the data as functions of the inputs. Figures 23, 24, 25 and 26 show the different properties of the carbon fiber-foam tested.

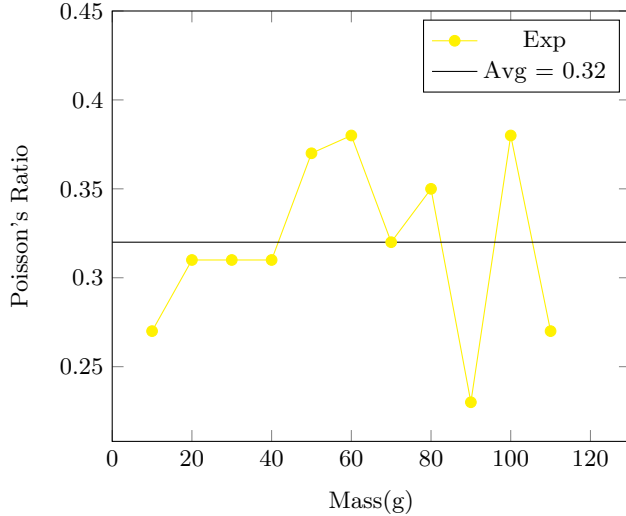


FIG. 23. **Poisson's Ratio vs. Mass.** A constant behavior should be observed as the Poisson's ratio stands for the change in the width per unit width of a material, to the change in its length per unit length, as a result of strain.

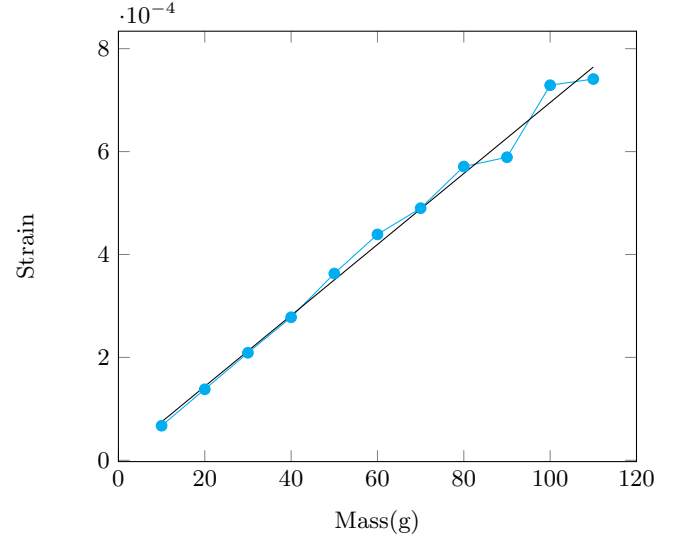


FIG. 24. **Strain vs. Mass.** A linear behavior is observed as the strain is proportional to the mass, indirectly through the stress.

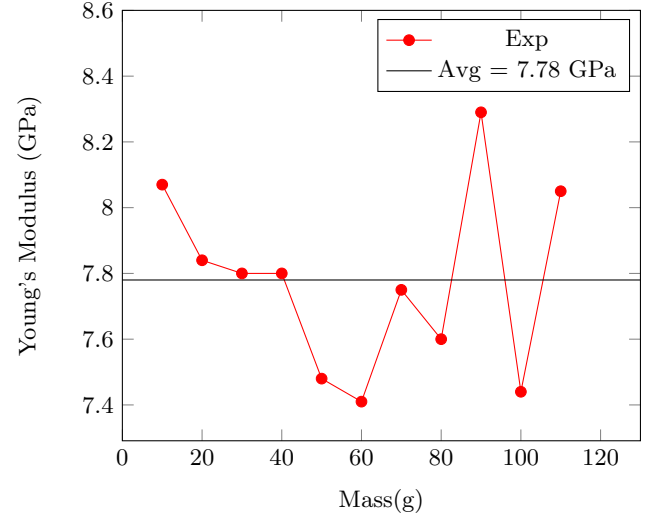


FIG. 25. **Young's Modulus vs. Mass.** A constant behavior should be observed as the Young's Modulus stands for the elasticity modulus, a constant property of materials.

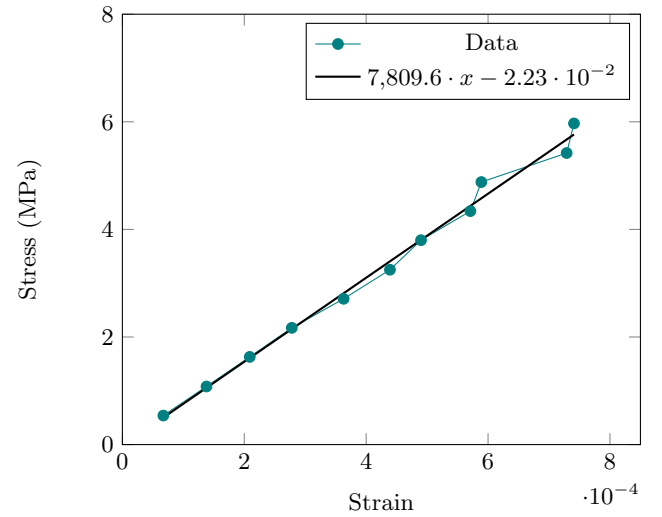


FIG. 26. **Stress vs. Strain.** A linear behavior is observed as the stress is proportional to the strain, as defined by the Young's modulus.

Additionally, for another carbon fiber-foam sample, the distance between the clamp and the mass was measured to be 87.0 mm. Using the 2-grid gauges of 350  $\Omega$  resistance in a full Wheatstone bridge configuration, wires with lead resistance of 12  $\Omega$ , and an initial source voltage of 0.5 V, approximately, the test results for this sample are shown next.

TABLE IX. Strain-Stress Test Results for Carbon Fiber-Foam in Full Bridge circuit.

Mass [g]	Voltage Ratio	Poisson's Ratio
10	-5.45e-05	0.42
20	-1.12e-04	0.46
30	-1.67e-04	0.45
40	-2.21e-04	0.45
50	-2.64e-04	0.38
60	-3.24e-04	0.41
70	-3.84e-04	0.43
80	-4.55e-04	0.49
90	-5.40e-04	0.57
100	-5.62e-04	0.47
110	-5.87e-04	0.39
120	-6.56e-04	0.43

Mass [g]	Strain	Stress [MPa]	Young's Modulus [GPa]
10	3.83e-05	0.29	7.57
20	7.66e-05	0.58	7.58
30	1.15e-04	0.86	7.49
40	1.53e-04	1.15	7.51
50	1.91e-04	1.44	7.52
60	2.30e-04	1.73	7.53
70	2.68e-04	2.02	7.54
80	3.06e-04	2.30	7.51
90	3.44e-04	2.59	7.52
100	3.83e-04	2.88	7.52
110	4.21e-04	3.17	7.53
120	4.59e-04	3.46	7.53

From these results, the average Poisson's ratio calculated was 0.45. This value was then implemented to the strain equation for computing once again the Young's modulus, resulting in an average modulus of 7.53.

Furthermore, to help visualize and understand these calculations, the following graphs plot the data as functions of the inputs. Figures 27, 28, 29 and 30 show the different properties of the carbon fiber-foam tested.

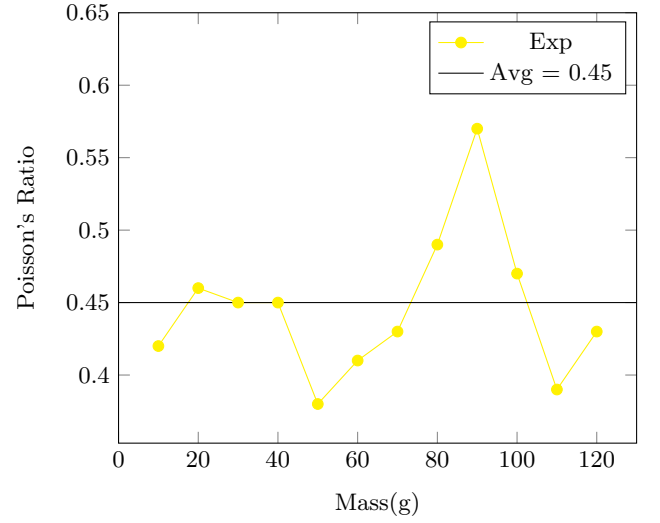


FIG. 27. **Poisson's Ratio vs. Mass.** A constant behavior should be observed as the Poisson's ratio stands for the change in the width per unit width of a material, to the change in its length per unit length, as a result of strain.

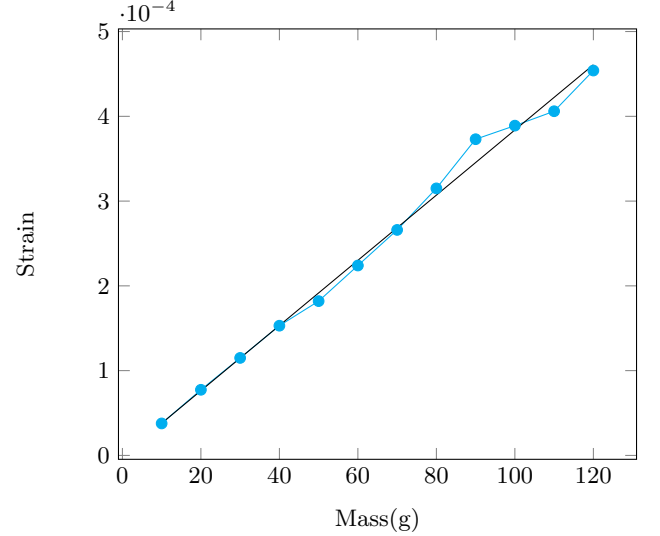


FIG. 28. **Strain vs. Mass.** A linear behavior is observed as the strain is proportional to the mass, indirectly through the stress.

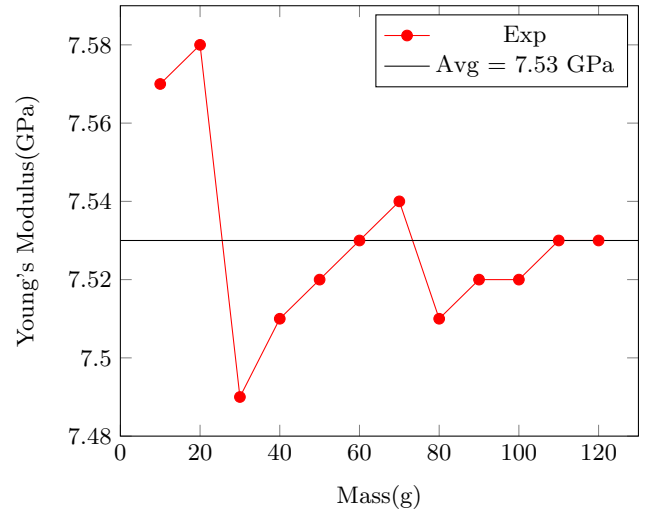


FIG. 29. **Young's Modulus vs. Mass.** A constant behavior should be observed as the Young's Modulus stands for the elasticity modulus, a constant property of materials.

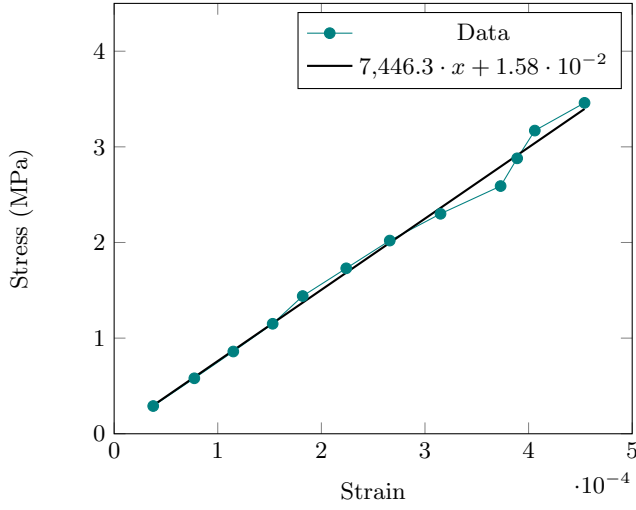


FIG. 30. **Stress vs. Strain.** A linear behavior is observed as the stress is proportional to the strain, as defined by the Young's modulus.

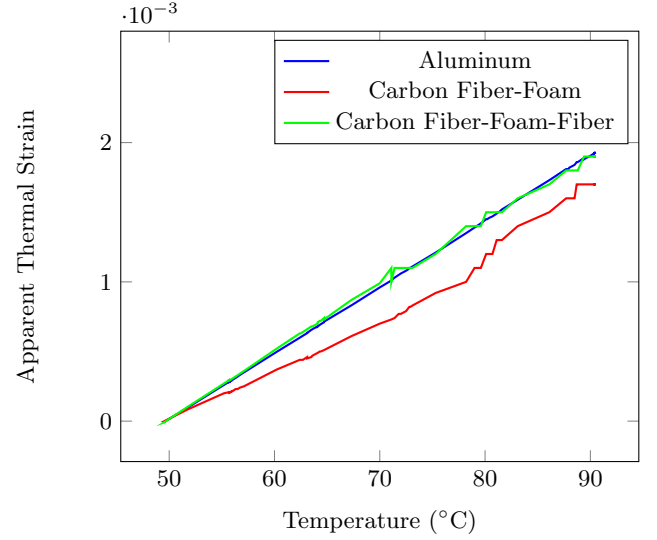


FIG. 31. **Strain vs. Temperature.** A linear behavior is observed as the strain is proportional to the increase of temperature, as defined by thermal shock.

### C. Thermal Expansion

Results of the thermal shock experiment were taken from the data logger and individually analyzed. The samples selected for testing are the aluminum, carbon fiber-foam and carbon fiber-foam-fiber described previously for the Half Bridge configuration. These test pieces would undergo a temperature change from the range of 30 °C - 110 °C, depending on the test run; in total three runs were performed.

The 3-grid gauges of 120  $\Omega$  resistance were connected in parallel giving an output resistance of 40  $\Omega$ . Using half Wheatstone bridge configuration for all three samples, wires with lead resistance of 12  $\Omega$ , and an initial source voltage of 0.5 V, approximately, the test results are shown below. Figures 31, 32 and 33 show the different performances of thermal strain for each sample tested.

TABLE X. **Run 1.** Apparent Thermal Strain Test Results for Aluminum (AL), Carbon Fiber-Foam (CF) and Carbon Fiber-Foam-Fiber (DCF) in Half Bridge circuit.

Temp [°C]	Strain (AL)	Strain (CF)	Strain (DCF)
51.7	9.46e-05	8.20e-05	1.00e-04
56.1	3.01e-04	2.20e-04	3.10e-04
60.2	4.97e-04	3.70e-04	5.20e-04
64.7	7.14e-04	5.10e-04	7.30e-04
70.0	9.60e-04	7.00e-04	9.90e-04
75.3	1.21e-03	9.20e-04	1.20e-03
80.1	1.45e-03	1.20e-03	1.50e-03
86.1	1.73e-03	1.50e-03	1.70e-03
90.3	1.92e-03	1.70e-03	1.90e-03

TABLE XI. **Run 2.** Apparent Thermal Strain Test Results for Aluminum (AL), Carbon Fiber-Foam (CF) and Carbon Fiber-Foam-Fiber (DCF) in Half Bridge circuit.

Temp [°C]	Strain (AL)	Strain (CF)	Strain (DCF)
30.8	1.44e-04	2.77e-03	7.94e-03
42.7	7.03e-04	3.19e-03	8.52e-03
52.2	1.16e-03	3.48e-03	8.99e-03
60.3	1.54e-03	3.72e-03	9.39e-03
70.2	2.02e-03	3.96e-03	9.89e-03
80.2	2.50e-03	4.24e-03	1.04e-02
91.5	3.03e-03	4.71e-03	1.09e-02
99.7	3.42e-03	5.12e-03	1.13e-02

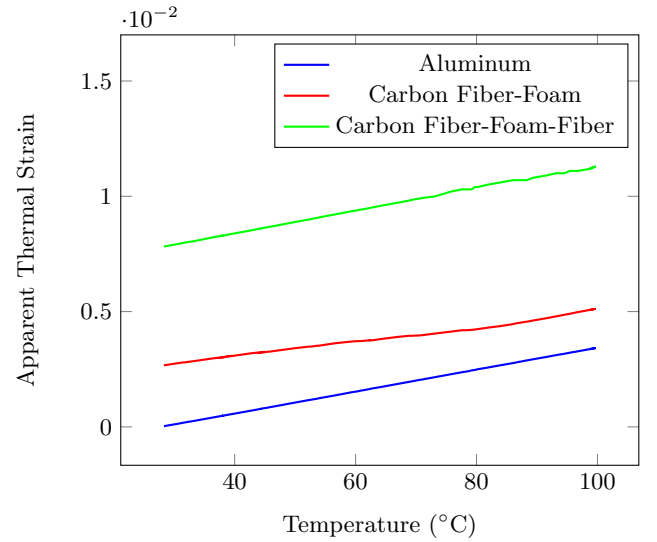


FIG. 32. **Strain vs. Temperature.** A linear behavior is observed as the strain is proportional to the increase of temperature, as defined by thermal shock.

TABLE XII. **Run 3.** Apparent Thermal Strain Test Results for Aluminum (AL), Carbon Fiber-Foam (CF) and Carbon Fiber-Foam-Fiber (DCF) in Half Bridge circuit.

Temp [°C]	Strain (AL)	Strain (CF)	Strain (DCF)
30.1	6.07e-06	2.51e-03	7.93e-03
40.1	1.42e-05	2.37e-03	7.95e-03
50.5	1.42e-05	2.22e-03	7.96e-03
60.9	1.21e-05	2.06e-03	7.99e-03
70.8	1.82e-05	1.83e-03	8.01e-03
80.4	2.02e-05	1.81e-03	7.98e-03
91.2	3.24e-05	1.83e-03	7.96e-03
100	5.47e-05	1.82e-03	7.97e-03

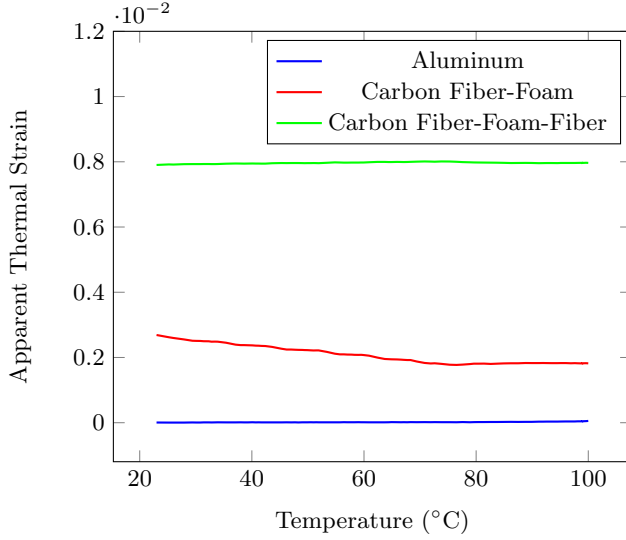


FIG. 33. **Strain vs. Temperature.** A linear behavior is observed as the strain is proportional to the increase of temperature, as defined by thermal shock.

Another thermal test involved using different Wheatstone Bridge configurations for carbon fiber-foam pieces. Figure 34 shows the thermal strain behavior for both samples tested. Interestingly, the results show that the carbon fiber-foam is contracting, instead of expansion as expected.

TABLE XIII. **Run 4.** Apparent Thermal Strain Test Results for Carbon Fiber-Foam in both Half and Full Bridge circuit.

Temperature [°C]	Strain (Half)	Strain (Full)
31.5	-6.84e-05	2.55e-04
43.1	-2.41e-04	1.15e-04
51.5	-3.74e-04	-2.01e-06
60.0	-5.01e-04	-9.05e-05
70.5	-6.39e-04	-1.51e-04
80.6	-6.61e-04	-1.65e-04
90.7	-5.69e-04	-2.37e-04
101.9	-5.07e-04	-3.44e-04
110.8	-4.97e-04	-3.98e-04

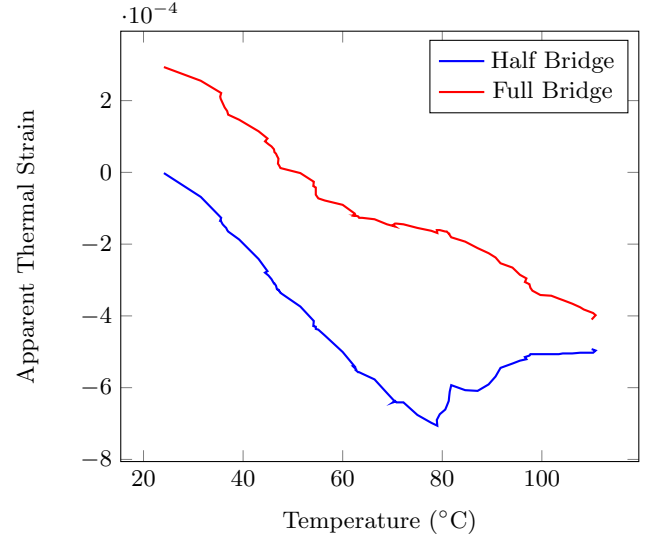


FIG. 34. **Strain vs. Temperature.** A linear behavior is observed as the strain is proportional to the increase of temperature, as defined by thermal shock, Carbon Fiber-Foam.

Additional thermal test results, including calculations for the thermal expansion coefficient, can be found in the Appendix B, at the end of the document.

## VII. CONCLUSIONS

The overall experiment was developed to measure the mechanical deformation and the thermal expansion of carbon-carbon composites. The main parameters of testing is an input force range of 0.1 to 1.2 N and temperature range from 30 to 110 °C. The experiment utilizes strain gauges to measure expansion and contraction of the materials and for measuring the temperature, a thermocouple. Measurements were made on aluminum, carbon fiber-foam and carbon fiber-foam-fiber with the means of measuring the Young's modulus, the Poisson's ratio and the thermal expansion coefficient of each one, along side with their strain and stress, mechanical or thermal. The method is particularly suitable for stress analysis in a laboratory, since it requires simple rather than special instrumentation or materials. Conceivably, the experiment procedure can be altered in order to extract the data with the utmost accuracy. From the results obtained and properties calculated can now profile the material in use. For the carbon fiber-foam, the Young's modulus is  $7.53 \pm 0.22$  GPa, the Poisson's ratio is  $0.32 \pm 0.13$ . For the carbon fiber-foam-fiber, the Young's modulus is  $96.5 \pm 4.50$  GPa.



## VIII. RECOMMENDATIONS

For further studies, I highly recommend taking caution with the gauge during the installation process, this will ensure the longevity of the test pieces. Additionally, plenty of calculations are necessary, and each equation differs slightly from the other, so double-check each pro-

cess. For the full Dee's test experiment, I would start test with half bridge configuration, even though some properties were calculated as described in the report above, the behavior of the material can change. For thermal experimentation, caution is your best ally, the expansion rate for the carbon-carbon composites is extremely sensitive.

- [1] N. Mahalik, in *Mems* (Tata McGraw-Hill Education, 2008) Chap. 3, pp. 102–104.
- [2] National Instruments, *Measuring Strain with Strain Gages*, <https://www.ni.com/en-us/innovations/white-papers/07/measuring-strain-with-strain-gages.html> (2019).
- [3] National Instruments, *Strain Gauge Measurement - A Tutorial*, [http://elektron.pol.lublin.pl/elekp/ap\\_notes/NI\\_AN078\\_Strain\\_Gauge\\_Meas.pdf](http://elektron.pol.lublin.pl/elekp/ap_notes/NI_AN078_Strain_Gauge_Meas.pdf) (1998), Application Note 078.
- [4] M. Gedeon, Cantilever beams, <https://materion.com/-/media/files/alloy/newsletters/technical-tidbits/issue-no-20--cantilever-beams---part-1-beam-stiffness.pdf> (2010), Issue No. 20.
- [5] Micro-Measurements, *Measurement of Thermal Expansion Coefficient Using Strain Gages*, [https://intertechnology.com/Vishay/pdfs/TechNotes\\_TechTips/TN-513.pdf](https://intertechnology.com/Vishay/pdfs/TechNotes_TechTips/TN-513.pdf) (2004), Technical Note 513.
- [6] KYOWA, Principles of self-temperature-compensation gages, [https://www.kyowa-ei.com/eng/technical/notes/technical\\_note/selcom\\_gages.html](https://www.kyowa-ei.com/eng/technical/notes/technical_note/selcom_gages.html).

## IX. APPENDIX A: STRAIN GAUGE INSTALLATION



FIG. 35. Mixing the epoxy X60.



FIG. 36. Applying glue to gauges.

## X. APPENDIX B: THERMAL EXPANSION RESULTS

Additional results of the thermal shock experiment were taken from the data logger and individually analyzed. The samples selected for testing are the aluminum, carbon fiber-foam and carbon fiber-foam-fiber described previously for the Half Bridge configuration. These test pieces would undergo a temperature change from the range of  $-20\text{ }^{\circ}\text{C}$  -  $180\text{ }^{\circ}\text{C}$ , depending on the test run; in total three runs were performed.

The 3-grid gauges of  $120\text{ }\Omega$  resistance were connected in parallel giving an output resistance of  $40\text{ }\Omega$ . Using half Wheatstone bridge configuration for all three samples, wires with lead resistance of  $12\text{ }\Omega$ , and an initial source voltage of  $0.5\text{ V}$ , approximately, the results for the thermal expansion coefficient ( $\alpha$ ) and thermal strain are shown below.

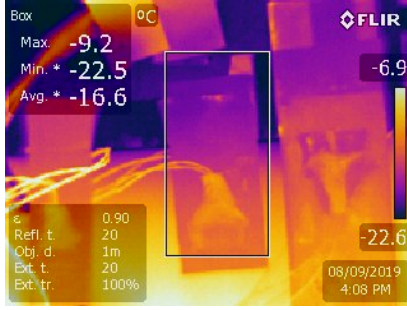


FIG. 37. Material samples inside Coldbox.

TABLE XIV. **Run 5.** Apparent Thermal Strain Test Results for Aluminum (AL), Carbon Fiber-Foam (CF) and Carbon Fiber-Foam-Fiber (DCF) in Half Bridge circuit.

Temp [ $^{\circ}\text{C}$ ]	$\alpha_{AL}$ [ $^{\circ}\text{C}^{-1}$ ]	$\alpha_{CF}$ [ $^{\circ}\text{C}^{-1}$ ]	$\alpha_{DCF}$ [ $^{\circ}\text{C}^{-1}$ ]
30.0	1.99e-06	1.56e-03	1.99e-06
40.1	1.53e-06	3.54e-04	1.99e-06
50.2	1.91e-06	1.89e-04	2.08e-06
60.1	1.67e-06	-1.12e-05	2.43e-06
70.1	1.66e-06	8.98e-06	2.38e-06
80.1	1.65e-06	5.50e-05	2.05e-06
90.0	1.49e-06	5.46e-05	1.47e-06
100.3	1.31e-06	2.91e-05	1.29e-06
110.0	1.22e-06	3.73e-05	1.29e-06
120.1	9.41e-07	1.55e-05	1.10e-06

Temp [ $^{\circ}\text{C}$ ]	Strain (AL)	Strain (CF)	Strain (DCF)
30.0	5.30e-05	4.82e-03	5.30e-05
40.1	6.70e-05	4.73e-03	7.30e-05
50.2	9.10e-05	4.46e-03	9.50e-05
60.1	1.02e-04	-3.29e-04	1.28e-04
70.1	1.18e-04	4.35e-04	1.50e-04
80.1	1.34e-04	2.98e-03	1.56e-04
90.0	1.40e-04	3.51e-03	1.40e-04
100.3	1.42e-04	2.19e-03	1.42e-04
110.0	1.48e-04	3.17e-03	1.54e-04
120.1	1.34e-04	1.50e-03	1.50e-04

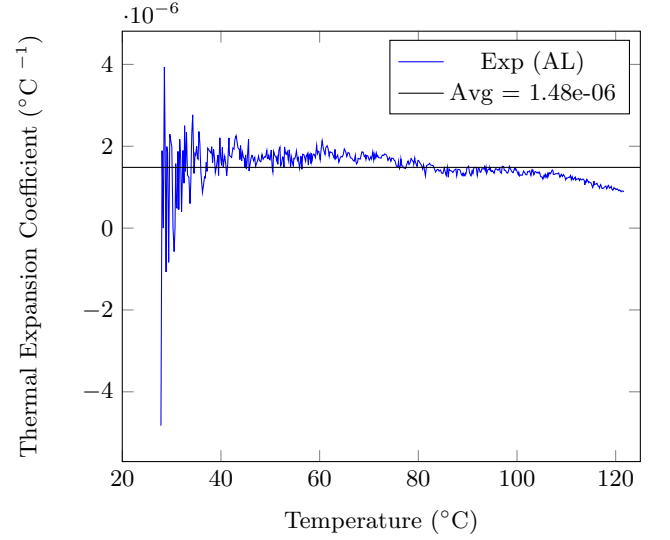


FIG. 38. **Thermal Coefficient vs. Temperature.** A constant behavior should be observed from this property.

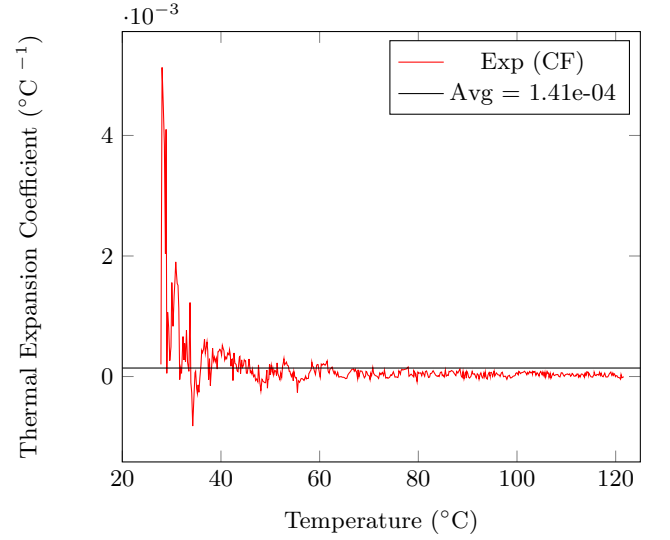


FIG. 39. **Thermal Coefficient vs. Temperature.** A constant behavior should be observed from this property.

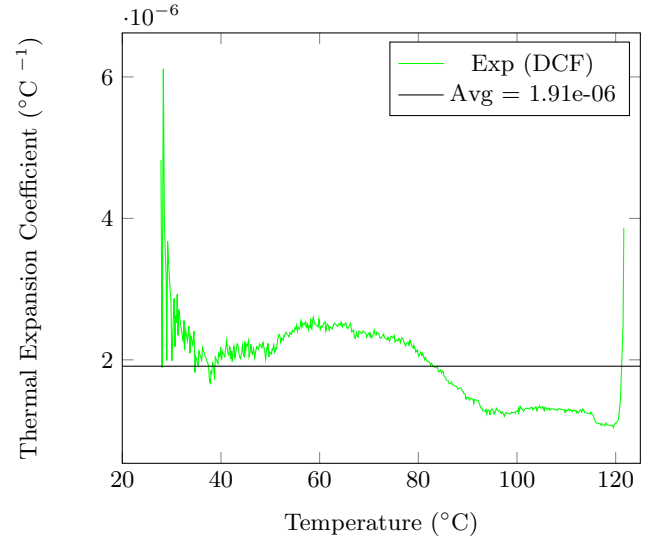


FIG. 40. **Thermal Coefficient vs. Temperature.** A constant behavior should be observed from this property.

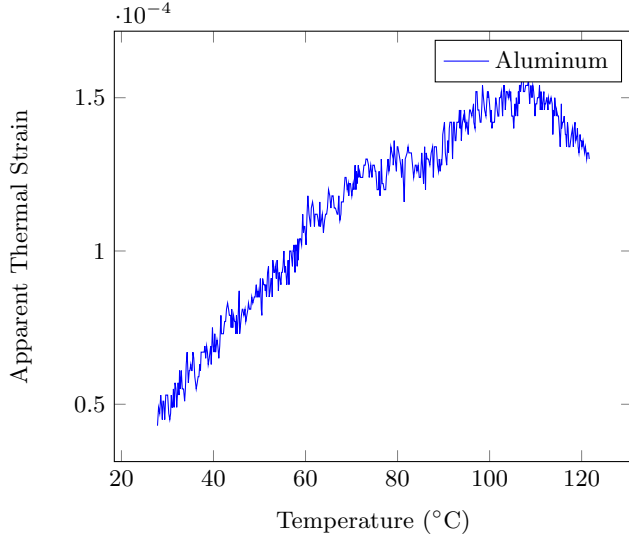


FIG. 41. **Strain vs. Temperature.** A proportional behavior from the strain due to temperature is observed.

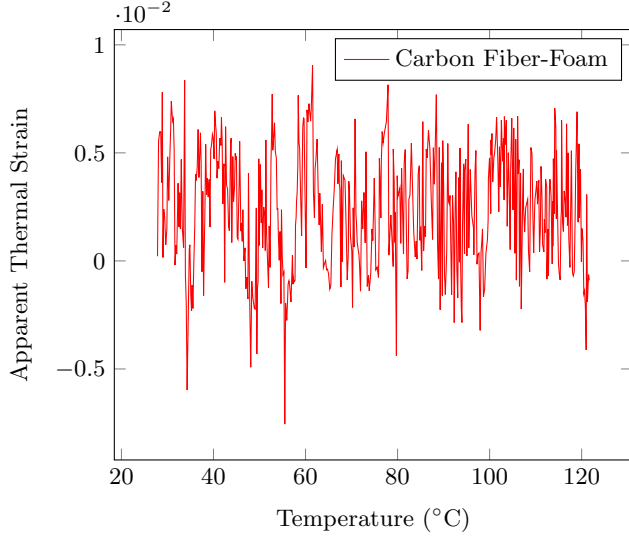


FIG. 42. **Strain vs. Temperature.** A proportional behavior from the strain due to temperature is observed.

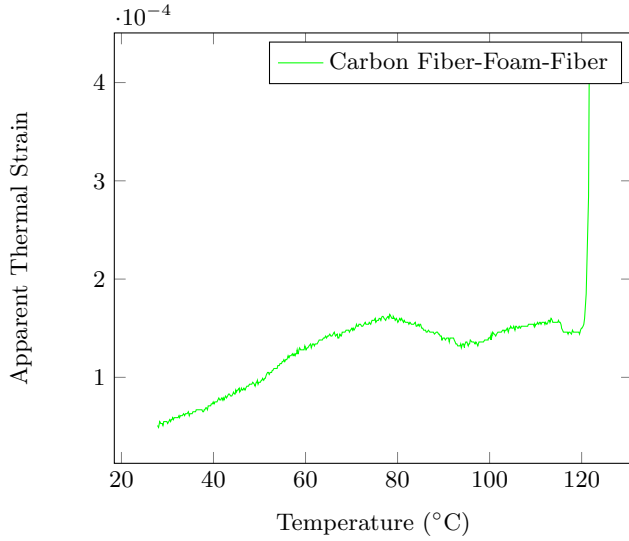


FIG. 43. **Strain vs. Temperature.** A proportional behavior from the strain due to temperature is observed.

TABLE XV. **Run 6.** Apparent Thermal Strain Test Results for Aluminum (AL), Carbon Fiber-Foam (CF) and Carbon Fiber-Foam-Fiber (DCF) in Half Bridge circuit.

Temp [°C]	$\alpha_{AL}$ [°C <sup>-1</sup> ]	$\alpha_{CF}$ [°C <sup>-1</sup> ]	$\alpha_{DCF}$ [°C <sup>-1</sup> ]
7.2	4.03e-05	-2.72e-04	0.00e+00
6.1	0.00e+00	6.50e-05	4.48e-06
5.0	0.00e+00	2.22e-05	2.02e-06
3.8	1.26e-06	1.26e-05	1.26e-06
2.9	4.92e-07	7.38e-06	9.84e-07
0.6	9.45e-07	3.15e-06	9.45e-07
-1.2	9.84e-07	-1.23e-06	7.38e-07
-3.0	4.03e-07	5.24e-06	1.01e-06
-4.1	-3.63e-07	-8.36e-06	1.27e-06
-5.1	1.67e-07	-7.00e-06	1.33e-06
-6.1	3.08e-07	-8.78e-06	1.08e-06
-7.1	5.72e-07	-9.44e-06	1.14e-06
-8.1	4.01e-07	-6.68e-06	9.35e-07
-9.1	3.76e-07	-6.89e-06	1.00e-06
-10.0	3.56e-07	-6.17e-06	8.31e-07
-11.0	3.36e-07	-6.05e-06	1.12e-06
-12.0	3.18e-07	-7.86e-06	7.43e-07
-13.0	4.03e-07	-9.18e-06	8.07e-07
-14.0	4.80e-07	-7.68e-06	5.76e-07
-15.0	5.50e-07	-9.63e-06	9.17e-07
-16.0	5.26e-07	-1.11e-05	7.02e-07
-17.0	4.20e-07	-1.03e-05	8.40e-07

Temp [°C]	Strain (AL)	Strain (CF)	Strain (DCF)
7.2	1.76e-05	-4.54e-05	9.46e-06
6.1	-4.26e-05	-1.01e-04	-4.66e-05
5.0	-9.46e-05	-1.39e-04	-9.87e-05
3.8	-1.55e-04	-1.92e-04	-1.55e-04
2.9	-1.96e-04	-2.24e-04	-1.98e-04
0.6	-3.09e-04	-3.23e-04	-3.09e-04
-1.2	-3.96e-04	-3.78e-04	-3.94e-04
-3.0	-4.77e-04	-4.20e-04	-4.83e-04
-4.1	-5.21e-04	-4.32e-04	-5.39e-04
-5.1	-5.75e-04	-4.87e-04	-5.89e-04
-6.1	-6.24e-04	-5.04e-04	-6.34e-04
-7.1	-6.75e-04	-5.33e-04	-6.83e-04
-8.1	-7.21e-04	-6.13e-04	-7.29e-04
-9.1	-7.68e-04	-6.50e-04	-7.78e-04
-10.0	-8.10e-04	-6.99e-04	-8.19e-04
-11.0	-8.58e-04	-7.42e-04	-8.72e-04
-12.0	-9.05e-04	-7.49e-04	-9.13e-04
-13.0	-9.54e-04	-7.61e-04	-9.63e-04
-14.0	-1.00e-03	-8.31e-04	-1.01e-03
-15.0	-1.05e-03	-8.28e-04	-1.06e-03
-16.0	-1.10e-03	-8.30e-04	-1.10e-03
-17.0	-1.15e-03	-8.86e-04	-1.16e-03

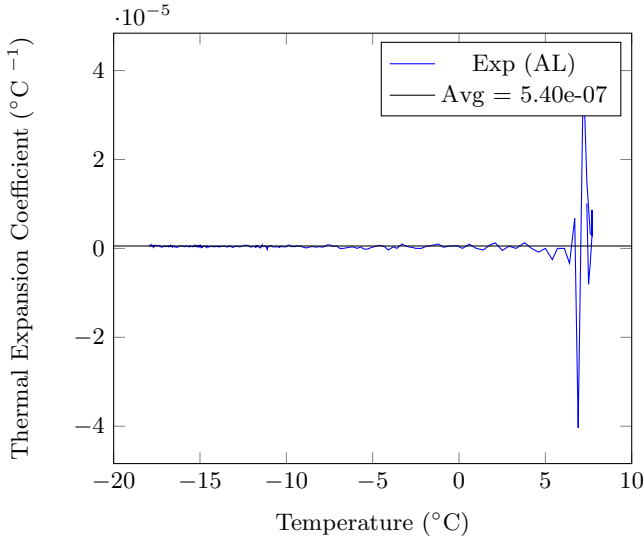


FIG. 44. **Thermal Coefficient vs. Temperature.** A constant behavior should be observed from this property.

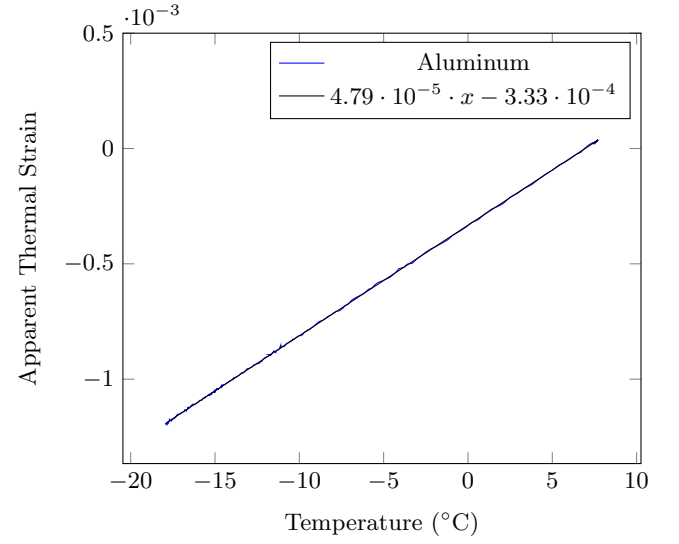


FIG. 47. **Strain vs. Temperature.** A proportional behavior from the strain due to temperature is observed.

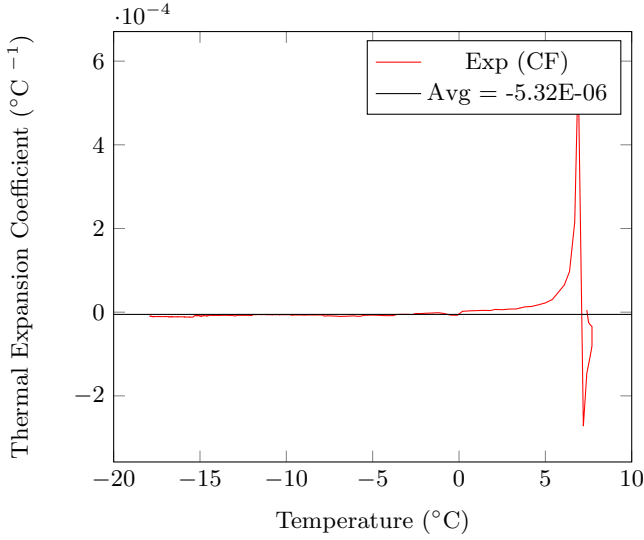


FIG. 45. **Thermal Coefficient vs. Temperature.** A constant behavior should be observed from this property.

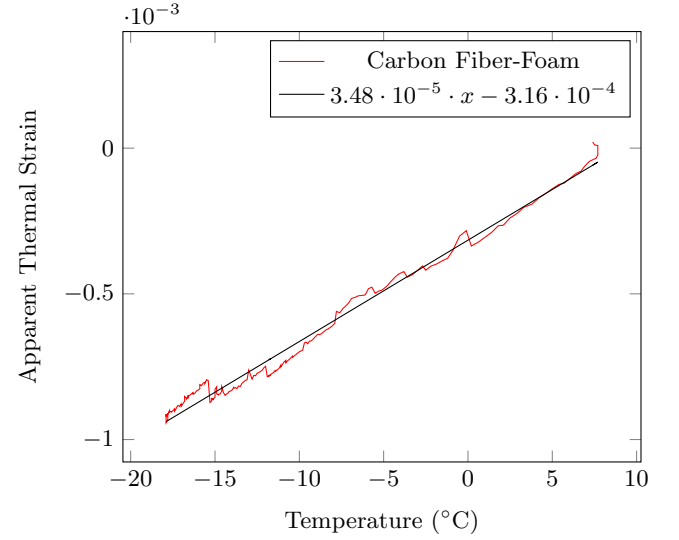


FIG. 48. **Strain vs. Temperature.** A proportional behavior from the strain due to temperature is observed.

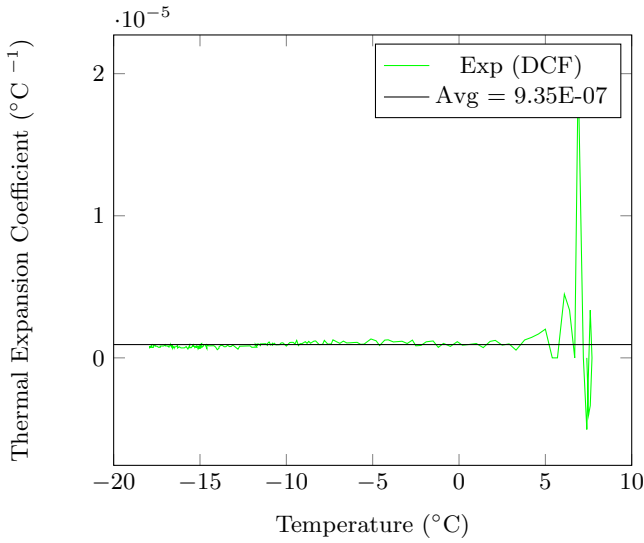


FIG. 46. **Thermal Coefficient vs. Temperature.** A constant behavior should be observed from this property.

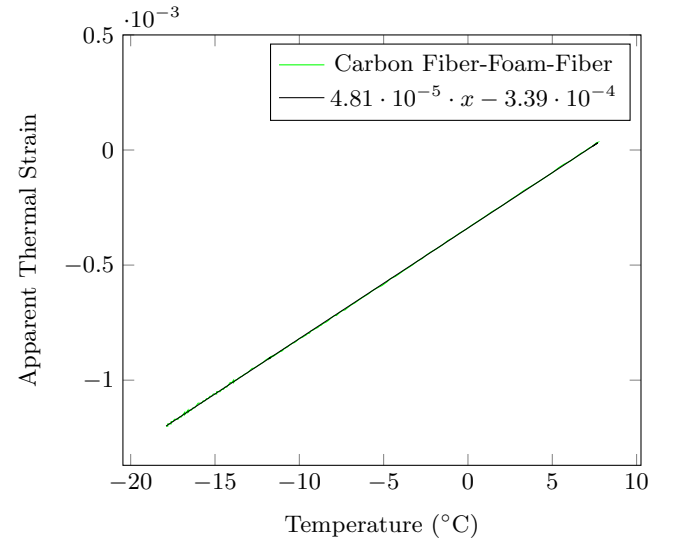


FIG. 49. **Strain vs. Temperature.** A proportional behavior from the strain due to temperature is observed.

TABLE XVI. **Run 7.** Apparent Thermal Strain Test Results for Aluminum (AL), Carbon Fiber-Foam (CF) and Carbon Fiber-Foam-Fiber (DCF) in Half Bridge circuit.

Temp [°C]	$\alpha_{AL}$ [°C <sup>-1</sup> ]	$\alpha_{CF}$ [°C <sup>-1</sup> ]	$\alpha_{DCF}$ [°C <sup>-1</sup> ]
30	3.28E-06	6.61E-04	2.52E-06
40	2.47E-06	4.12E-04	2.80E-06
50	2.02E-06	2.14E-04	3.03E-06
60	2.07E-06	1.36E-04	3.29E-06
70	1.81E-06	1.55E-04	3.28E-06
80	1.50E-06	2.11E-04	3.20E-06
90	1.36E-06	1.73E-04	2.58E-06
100	9.83E-07	1.07E-04	4.42E-06
110	7.56E-07	9.45E-05	4.93E-06
120	6.79E-07	1.09E-04	7.35E-06
130	4.86E-07	6.22E-05	9.12E-04
140	2.91E-07	6.90E-05	8.34E-04
150	9.45E-08	5.68E-05	7.69E-04
160	-4.38E-08	4.95E-05	2.09E-06
170	4.50E-07	6.62E-05	2.77E-06

Temp [°C]	Strain (AL)	Strain (CF)	Strain (DCF)
30	3.67E-05	5.33E-03	3.06E-05
40	6.78E-05	7.49E-03	7.39E-05
50	9.28E-05	6.06E-03	1.21E-04
60	1.28E-04	5.25E-03	1.75E-04
70	1.49E-04	7.54E-03	2.20E-04
80	1.62E-04	1.24E-02	2.61E-04
90	1.81E-04	1.20E-02	2.64E-04
100	1.77E-04	8.49E-03	4.47E-04
110	1.80E-04	8.48E-03	5.50E-04
120	1.93E-04	1.09E-02	8.51E-04
130	1.91E-04	6.90E-03	9.93E-02
140	1.86E-04	8.34E-03	9.92E-02
150	1.76E-04	7.48E-03	9.93E-02
160	1.71E-04	7.05E-03	4.67E-04
170	2.57E-04	1.00E-02	6.02E-04

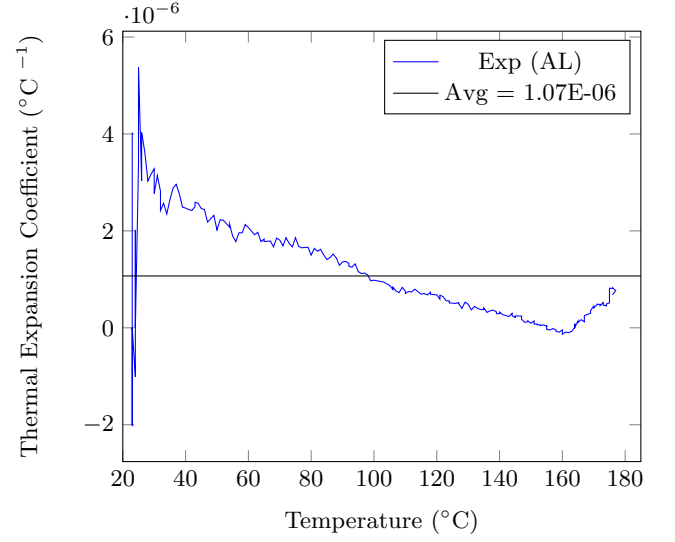


FIG. 50. **Thermal Coefficient vs. Temperature.** A constant behavior should be observed from this property.

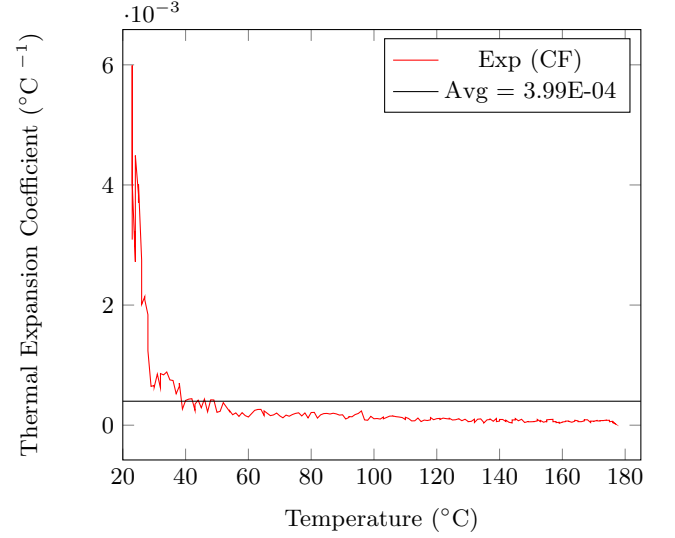


FIG. 51. **Thermal Coefficient vs. Temperature.** A constant behavior should be observed from this property.

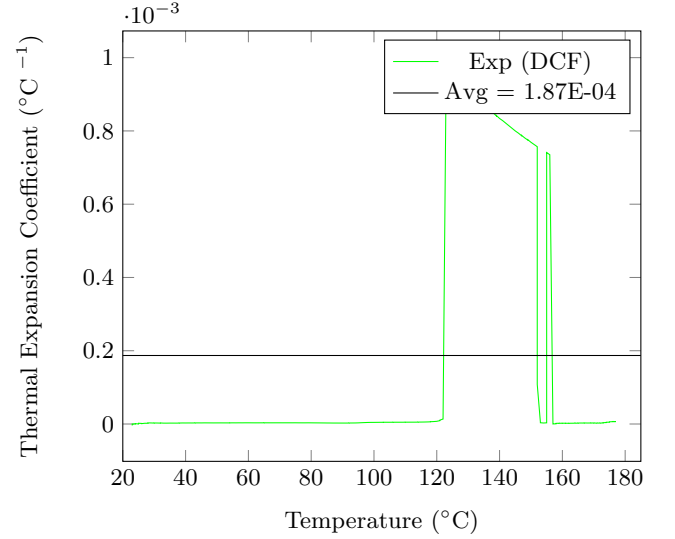


FIG. 52. **Thermal Coefficient vs. Temperature.** A constant behavior should be observed from this property.



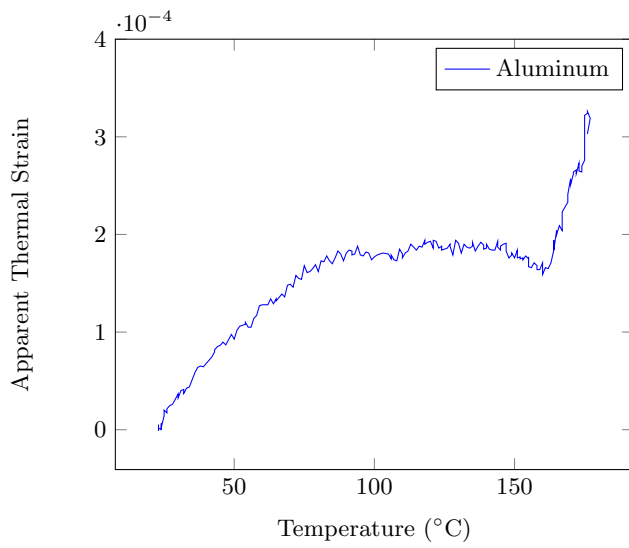


FIG. 53. **Strain vs. Temperature.** A proportional behavior from the strain due to temperature is observed.

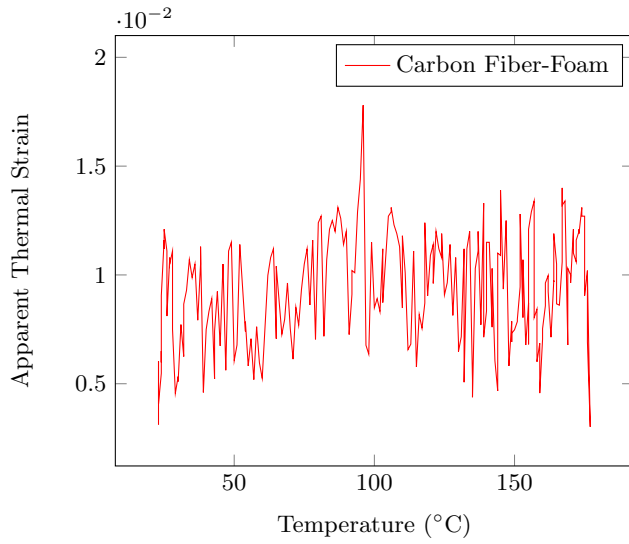


FIG. 54. **Strain vs. Temperature.** A proportional behavior from the strain due to temperature is observed.

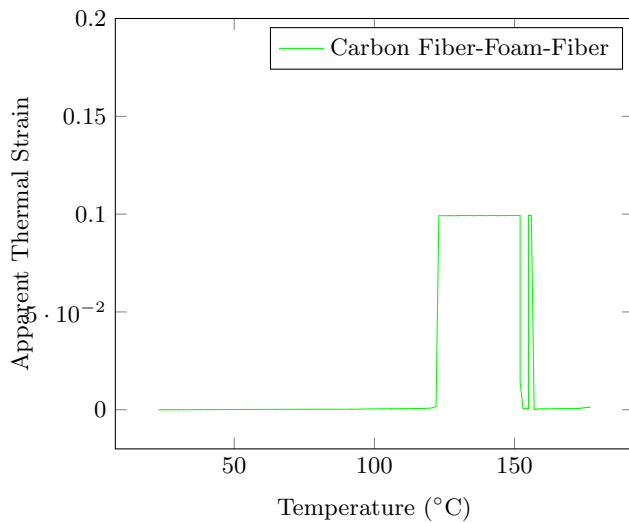


FIG. 55. **Strain vs. Temperature.** A proportional behavior from the strain due to temperature is observed.